A Hybrid Variable *m*-CAP-Based Indoor Visible Light Communications and Fingerprint Positioning System

Mahdi Nassiri
Department of Electrical Engineering
University of Guilan
Rasht, Iran
nassiri@msc.guilan.ac.ir

Atiyeh Pouralizadeh
Department of Electrical Engineering
University of Guilan
Rasht, Iran
atiyehpouralizadeh@gmail.com

Gholamreza Baghersalimi
Department of Electrical Engineering
University of Guilan
Rasht, Iran
bsalimi@guilan.ac.ir

Zabih Ghassemlooy
Optical Communications Research Group, Faculty of Engineering and Environment
Northumbria University
Newcastle, UK
z.ghassemlooy@northumbria.ac.uk

***Abstract*—a variable multi-band carrier-less amplitude and phase (*m*-CAP)-based indoor hybrid visible light link for data communications and positioning is investigated in this paper. Here, we have adopted the fingerprinting algorithm for positioning. Both the link performance in terms of the bit error rate (BER) and the positioning error (PE) are evaluated for a range of E_b/N_0 and step sizes for the data communications and localization, respectively. Results show that, the best PE value and the spectral efficiency of the proposed system are ~2 cm and 6.15 b/s/Hz with respect for a step size of 2 cm and a 7% forward error correction BER limit of 3.8×10^{-3}, respectively.**

Keywords—visible light communications, indoor positioning, variable m-CAP, fingerprinting

I. Introduction

New high data rate multimedia services and applications are developing extremely, which highlight the shortage of capacity in fifth generation (5G) and beyond wireless networks. The growth in data rate is creating a major challenge in existing radio frequency (RF)-based wireless technologies known as spectral congestion, which needs addressing. In addition, the RF technologies have other drawbacks such as lower data rates, costly spectrum licensing, security and high installation cost [1, 2]. Alternatively, optical wireless communications (OWC) including infrared, visible and ultraviolet spectrum bands offers features, which are complementary to RF, and can be used in a range of applications, thus releasing the pressure on the RF usage. Some attractive features of OWC include license free, virtually unlimited bandwidth for providing near-optimal capacity, a green technology with a high energy efficiency, security and low installation costs [1, 3]. Visible light communications (VLC) refer to OWC systems working in the visible light band, i.e., 370-780 nm, which has attracted intensifying research interests in the last decade [4-6]. VLC is based on the principle of modulating the intensity of light emitting diodes (LEDs) without any harmful effects on the human eye and the light intensity. This opens up the opportunity for exploiting LED-based lighting infrastructure for illumination, wireless data communication, sensing and indoor positioning [7]. The latter is one most interesting feature of VLC that can be used in many applications.

As the number of smart mobile devices users is increasing, the need for development of a range of highly accurate location-based services and application based on the user's location is growing. In the literature, the importance of positioning schemes accurately determining the current location of a user has been reported [8-10]. To enumerate some potential fields of indoor positioning systems (IPSs) with centimeter level accuracy, can mention to different field such as marketing, healthcare, manufacturing, automation in buildings and so on. Applications include (*i*) staff location detecting; (*ii*) asset tracking; (*iii*) aiding visually impaired people in hospitals and in large indoor areas; and (*iv*) guiding robots for pick and place [11, 12].

The positioning systems are generally classified for outdoor and indoor applications. The outdoor positioning technology based on the global positioning system (GPS) cannot be used in indoor environments (e.g., tunnels, undergrounds and shopping centers, hospitals, etc.). This is due to the GPS signals with high dependency on the line-of-sight (LOS) transmission path are subjected to diffraction and reflection by buildings and cannot penetrate them. Additionally, GPS offers an accuracy of a few meters, which is sufficient for outdoor applications but not for indoor [12]. To solve the restraints of GPS in indoor environments, a number of signal-based technologies such as ultra wide band (UWB), ultrasonic wave, wireless local area networks (WLAN), Wi-Fi [13], Bluetooth [14], radio frequency identification (RFID) [15], ZigBee [16], inertial sensors-based localization [17] and visible light positioning (VLP) have been proposed. Among them, the VLP using LED lights with very low positioning error (PE) compared with Wi-Fi and Bluetooth is seen as a viable candidate [18]. Wireless IPSs are classified into four categories: (*i*) received signal strength (RSS); (*ii*) time of arrival (TOA); (*iii*) angle of arrival (AOA); and (*iv*) advanced filters. RSS values has been broadly used in VLP and is also adopted in this work due to its easy extraction by a simple photodiode (PD) without the demand for an extra device. Accordingly, different algorithms such as trilateration, proximity and fingerprinting have been developed for VLP to achieve improved performance [18, 19]. However, there are still some challenges, which needs addressing.

A large number of LEDs with the purpose of illumination are used in in many indoor environments, which cover the entire space, and can be used as transmitters (Txs). In places the illumination areas overlap, which is fine from the illumination point of view, but can induce to inter-cell interference (ICI) in data transmission if all the Txs use the same frequencies [19]. One of the most common approaches for combating the ICI in VLC is the use of multi-carrier modulation such as orthogonal frequency division multiplexing (OFDM). For instance, in [20] a minimum of three sub-bands (SBs) and therefore three LEDs were used for IPS with a mean PE of 1.3 cm and no ICI, which is considerably lower compared with the GPS system. However, the OFDM-based VLC system with a high peak-to-average power ratio (PAPR) is sensitive to the nonlinearity of the LEDs, which is the main reason to the system performance declining.

Recently, carrier-less amplitude and phase (CAP) modulation, as a surrogate to OFDM, has been proposed for VLC, where the carrier frequencies are produced by simple and cost-efficient finite impulse response (FIR) filters. In CAP (*i*) there is not any fast Fourier transform (FFT) and inverse FFT (IFFT) as in OFDM, which reduces the complexity of the VLC system; and (*ii*) is more robust against the LED nonlinearity given that PAPR values are lower compared with OFDM [21]. Nevertheless, a flat frequency response, which is required for optimal CAP performance, represents a substantial challenge towards implementing CAP in VLC. As a solution for this issue, a multi-band CAP (*m*-CAP) scheme was introduced by splitting the available bandwidth into *m* equally spaced SBs to relax the flat band response [22, 23].

The main idea of what is being proposed in this paper is based on the our previous work in [24], where we proposed a fingerprinting-based hybrid VLP and VLC system using *m*-CAP modulation for the first time. In this study, the focus is on VLC-IPS, where the first SB of a variable $4_{1/3}$-CAP is allocated for VLC, whereas the remaining SBs are assigned for positioning information and less important data transmission such as advertising data.

The rest of the paper is organized as follows. Section II provides an overview of the fingerprinting visible light-based IPS using variable *m*-CAP modulation. Results and discussion are presented in Section III. Eventually, Section IV is assigned to conclude the paper.

II. System Overview

Fig. 1 shows the schematic system block diagram of the of the proposed $4_{1/3}$-CAP hybrid VLC-VLP system. As shown, three $4_{1/3}$-CAP modules are used where three SBs are assigned for data transmission and a single SB is allocated for positioning (as an example for the first module: D_1, D_2 and D_3 for VLC, and P_1 for VLP). Note that, at least three LEDs are required as the Txs to achieve accurate positioning. Since the focus of this paper is on VLC, the 1st SB of each variable $4_{1/3}$-CAP module is considered for data transmission (i.e., D_1, D_4 and D_7), where 16-quadrature amplitude modulation (16-QAM) is adopted. Note the followings: (*i*) the 1st SB bandwidth B_{SB} of each variable $4_{1/3}$-CAP module is equal to the modulation bandwidth of LED B_{mod}, thus the 1st B_{SB} is three times larger than the bandwidth of other SBs in this work, see Fig. 2; (*ii*) P_1, P_2 and P_3 (i.e., the positioning indices of Tx_1, Tx_2 and Tx_3, respectively) are

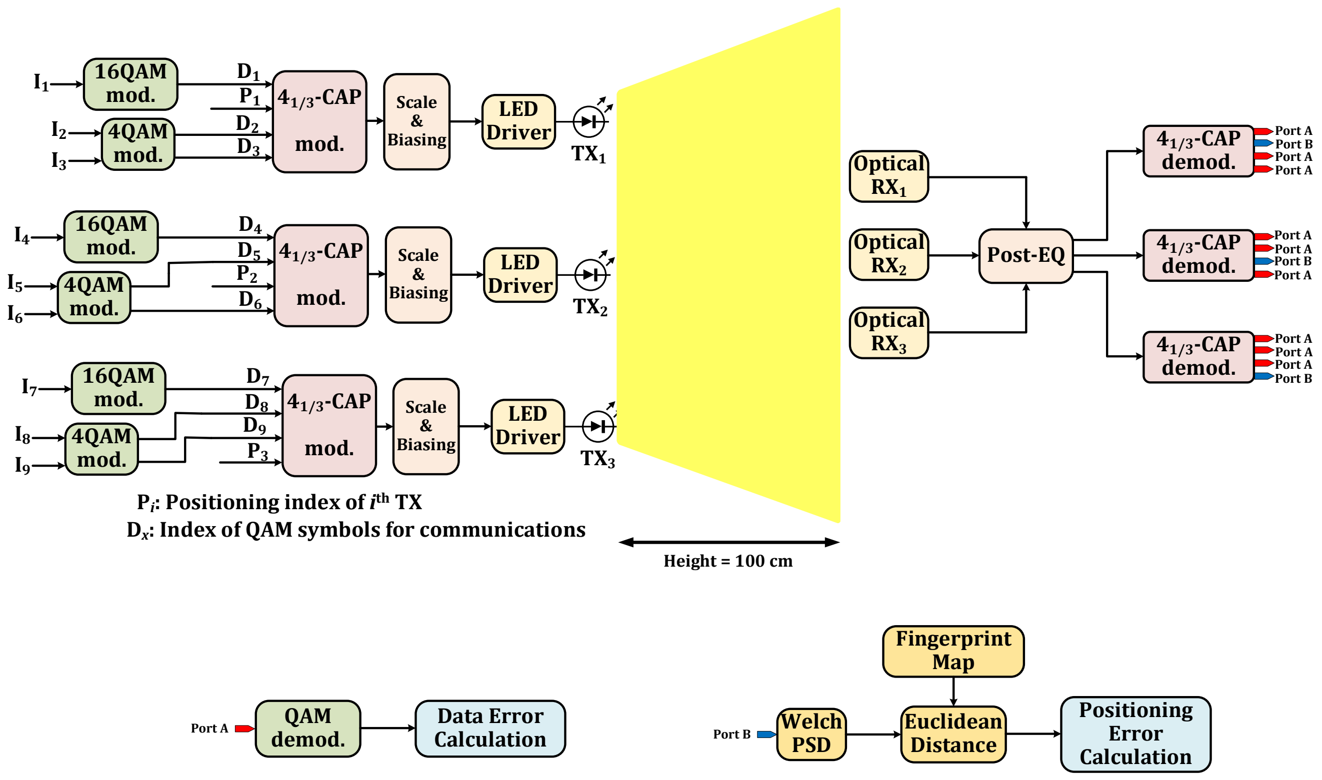

Fig. 1. Schematic diagram of the proposed variable *m*-CAP-based hybrid VLC-VLP system.

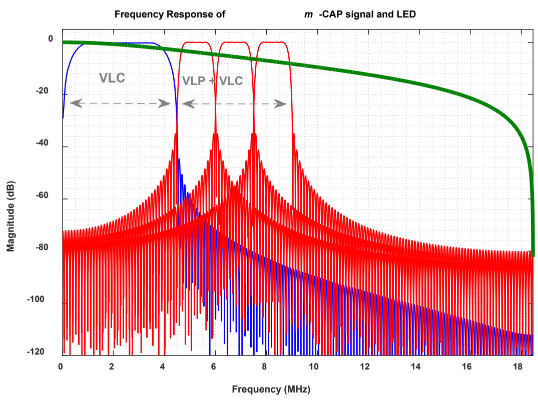

Fig. 2. Frequency representation of the proposed variable $4_{1/3}$-CAP.

inserted at 2nd, 3rd and 4th SBs of the variable $4_{1/3}$-CAP modules 1, 2 and 3, respectively to avoid interference at the receiver (Rx) side; (*iii*) other SBs with 4-QAM (i.e., D_2, D_3, D_5, D_6, D_8 and D_9) are assigned for transmission of lower data rates such as advertising data in order to improve the spectral efficiency. As mentioned before, for conventional *m*-CAP systems, the total signal bandwidth B_T is divided into *m* equally distributed SBs. In [25], for the first time, B_{SB} was set such that the 1st SB is the same as B_{mod}, and subsequently the remaining bandwidth was distributed equally between (*m*-1) SBs. The results showed a considerable reduction in complexity due to decreasing the number of FIR filters by 80%, 75%, ~67% and 50% in contrast to the conventional 10-, 8-, 6- and 4-CAP, respectively. Fig. 2 illustrates this concept for m = 4. The 1st SB is always set to B_{mod} to guarantee relaxing of the flat frequency response requisite for the 1st SB. The rest of B_T is equally broke into (*m*-1) parts as given by [25]:

$$B_{SB}^{n} = \begin{cases} \dfrac{B_T}{2}, & n = 1 \\ \dfrac{B_T - \dfrac{B_T}{2}}{m-1}, & 2 \le n \le m \end{cases}, \quad (1)$$

where B_{SB}^{n} is the bandwidth of nth SB. The mapped complex data is up-sampled by means of zero padding and then the resultant signal is split into in-phase (*I*) and quadrature (*Q*) components before being passed through *I*/*Q* square root raised cosine (SRRC) filters. Finally, all SBs are summed together to form the $4_{1/3}$-CAP signal, which is given as [26]:

$$S(\mathrm{t}) = \sum_{n=1}^{4} \left(d_I^{n}(t) \otimes f_I^{n}(t) - d_Q^{n}(t) \otimes f_Q^{n}(t) \right), \quad (2)$$

where $d_I^{n}(t)$ and $d_Q^{n}(t)$ are the *I*/*Q* components of baseband data, respectively and $\otimes$ denotes the time domain convolution. Also, $f_I^{n}(t)$ and $f_Q^{n}(t)$ are *I*/*Q* SRRC filters impulse response, respectively. The outputs of the variable *m*-CAP modules are then used for intensity modulation (IM) of LEDs via the bias-tee and drivers modules. Three LEDs with B_{mod} of 4.5 MHz are used for illumination, data communications and positioning based on the best LEDs configuration in [24], i.e. lowest PE and bit error rate (BER).

At the Rx side following transmission through a 3×3 LOS VLC link, we have used three optical Rxs, each comprised of a single PD and a trans-impedance amplifier (TIA) to reconstruct the electrical signal. The zero-forcing (ZF) time domain post-equalizer is employed to ameliorate the inter-symbol interference (ISI) and ICI due to the limited B_{mod} and the multiple-input multiple-output channel, respectively. The equalized signals are applied to $4_{1/3}$-CAP demodulation modules to separate the SBs. The frequency contents of SBs related to the positioning information (port **B** in Fig. 1) are extracted using Welch power spectral density (PSD) [27] and compared with the values recorded already in the fingerprint map by Euclidean distance criterion to estimate PE. In addition, SBs associated with the data transmission (port **A** in Fig. 1) are applied to QAM demodulation with its output compared with I_1 to I_9 bit-stream to determine the BER.

The fingerprinting method is more accurate compared with trilateration and other technologies to provide localization, which can be carried out in two phases of offline training and online location estimation [28]. However, (*i*) the preliminary step of offline fingerprinting map construction is needed at the cost of increased time and efforts; and (*ii*) reconstruction of the fingerprint map whenever there are changes in indoor features (i.e., walls, furniture, etc.). In the offline stage the room is divided into a self-defined grid containing several pixels. On selecting a position of interest from the movement path, the training user's device collects a fingerprint of the 2D location (*x*, *y*), in the form of the RSS values of all three LEDs (i.e., f_1, f_2 and f_3), which are stored in a memory so-called the fingerprint map. To reduce the computation time, a suitable grid size (or step size Δ*g*) should be adopted. In the online stage, Euclidean distance is mostly used to ascertain the difference between the measured RSS values (i.e., f_1', f_2' and f_3') and those obtained from the fingerprint database, which is given as [24]:

$$d_{\mathrm{euc}}^{i} = \sqrt{\left(f_1^{i} - f_1^{'}\right)^2 + \left(f_2^{i} - f_2^{'}\right)^2 + \left(f_3^{i} - f_3^{'}\right)^2}. \quad (3)$$
$$\text{for} \quad 1 \le i \le MN$$

Let L and W be the length and width of the room, respectively M = $W/\Delta g$ and N = $L/\Delta g$. Following determining Euclidean distances, the coordinates of closest point can be easily identified as an estimation of the Rx's location.

III. Results and Discussions

In this section, the performance of the proposed hybrid $4_{1/3}$-CAP VLC-VLP system is investigated by means of computer simulation using MATLAB. The adopted key system parameters are summarized in Table I.

Fig. 3 illustrates the average BER as a function of E_b/N_0 for the $4_{1/3}$-CAP VLC link. As can be observed, the target 7% forward error correction (FEC) BER limit of 3.8×10^{-3} is achieved at E_b/N_0 > ~20 dB. Also shown in inset are the received constellation diagrams for all four SBs at E_b/N_0 of 20 dB. As mentioned before, the 1st SB of each $4_{1/3}$-CAP module is allocated for data transmission in 16-QAM format.

TABLE I. PROPOSED SYSTEM PARAMETERS

Symbol	Parameter	Value
-	Room size	180×120×100 cm^3
$\varphi_{1/2}$	Semi-power half angle	70°
ψ_c	PD field of view	60°
A	PD detector area	15 mm^2
d_{PD}	Distance between PDs	5 cm
B_{PD}	3-dB bandwidth of PD	30 MHz
R	Responsivity of PD	0.54 A/W
m	Number of SBs	4
B_{mod}	LED 3-dB bandwidth	4.5 MHz
β	Roll-off factor of I/Q filters	0.3
L_f	I/Q filters length	10 Sym.
B_T	Total bandwidth	9 MHz
B_{SB}^n	Bandwidth of n^{th} SB	4.5 MHz for $n = 1$ 1.5 MHz for $n \neq 1$
D_x	Modulation type	4- and 16-QAM
P_1	Positioning index of Tx$_1$	$-1 - i$
P_2	Positioning index of Tx$_2$	$1 + i$
P_3	Positioning index of Tx$_3$	$1 - i$
Δg	Step size	2, 5, and 10 cm
-	LEDs position	Tx$_1$: (60, 40, 100) Tx$_2$: (60, 80, 100) Tx$_3$: (120, 60, 100)
N_t	Number of LEDs	3
N_r	Number of PDs	3

The high quality of the 1st constellation diagram indicates the impact of being within the pass-band region of LED. Also, the constellation diagrams for the 2nd, 3rd and 4th SBs for each $4_{1/3}$-CAP module with 4-QAM show performance deterioration with the increasing order of m. Of course, the signal experiences higher attenuation within the stop-band (i.e., beyond B_{mod}).

One of the most challenging issues in fingerprinting-based positioning systems is selecting the optimum Δg to ensure minimum PE. In order to evaluate the performance of the proposed method, a room floor with the area of 180×120 cm^2 is divided into a 90×60, 36×24 and 18×12 grids with Δg of 2, 5 and 10 cm, respectively. Next, Euclidean distance between the measured RSS values and each triplet in the fingerprint map is calculated. The estimated position of the Rx is the smallest Euclidean distance in the fingerprint map. Fig. 4 demonstrates the PE as a function of E_b/N_0 for Δg of 2, 5 and 10 cm. As can be seen, the PE increases with Δg and deceases E_b/N_0. This is because, increasing Δg results in reduced number of pixels, thus leading to higher quantization errors. It is worth mentioning that the smaller Δg can lead to lower PE, but at the cost of higher level of computational complexity.

Finally, in Fig. 5(a), the actual and estimated positions of the Rxs are visually illustrated for the proposed system with fingerprinting algorithm and Δg of 2 cm. Fig. 5(b) depicts the PE for a number of points of the room, varying in order to the uneven light intensity levels. As shown, the maximum and minimum PE values of 8.43 and 1.02 cm are observed for Δg and E_b/N_0 of 2 cm and 20 dB, respectively at the corner and center of the room, respectively. Note that, the average PE is still ~1.86 cm for this case. As a deduction, it is advantageous to compare the PE and spectral efficiency (i.e., $\eta_{se} = k_{avg}N_t / (1+\beta)$), where k_{avg} is the average bits/symbol in the total $4_{1/3}$-CAP signal, in this work with our previous results [24]. In [24], only two out of five SBs with binary phase shift keying was allocated to the single-input

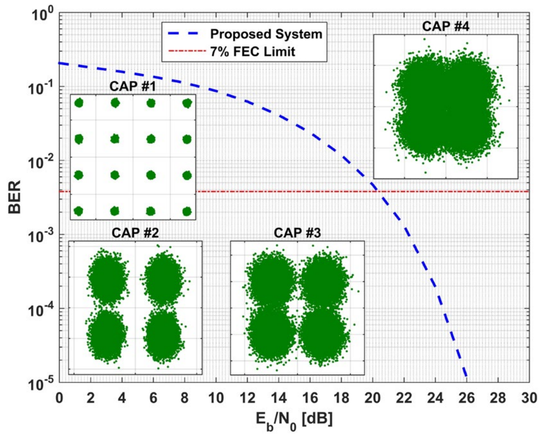

Fig. 3. Average BER performance vs. E_b/N_0 for the proposed $4_{1/3}$-CAP VLC link.

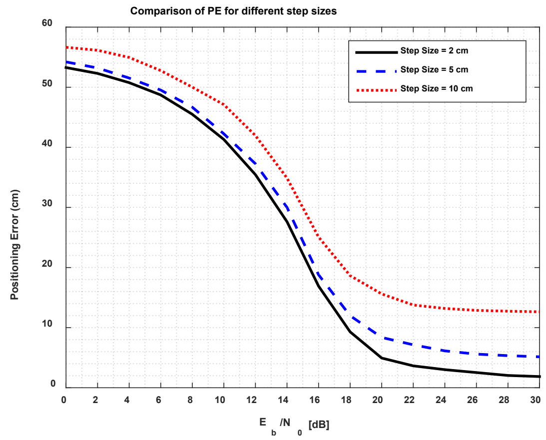

Fig. 4. The PE performance vs. E_b/N_0 and for different step sizes.

single-output VLC branch, thus k_{avg} and N_t were 2/5 = 0.4 and 1, respectively. For $\beta = 0.5$ we have $\eta_{se} \approx 0.27$ b/s/Hz as in [24], while in this study for $k_{avg} = 2.67$, $N_t = 3$, and $\beta = 0.3$ η_{se} is increased to 6.15 b/s/Hz. Nevertheless, this improvement takes precedence over increased PE from 2.66 to 5.15 cm for Δg of 5 cm as an example.

IV. CONCLUSION

In this paper, the variable m-CAP based indoor hybrid VLC and VLP system was propounded and assessed using the fingerprinting algorithm. We investigated the performance of the VLC link based bit error rate and achieved the 7% forward error correction limit at E_b/N_0 of ~20 dB. Also, we showed that, the positioning error increased with the step size, which is the most vital factor in fingerprinting-based positioning systems, for a fixed value of E_b/N_0. For instance, at the E_b/N_0 of 20 dB the PE values were 4.94 and 15.6 cm for the step sizes of 2 and 10 cm, respectively. In contrast, for a fixed step size the PE decreased with increasing E_b/N_0. Finally, it was shown that, PE values were not the same for different locations of the room since the light intensity at the corners and center of the room varied. Therefore, we adopted the average PE for all points to assess the system performance.

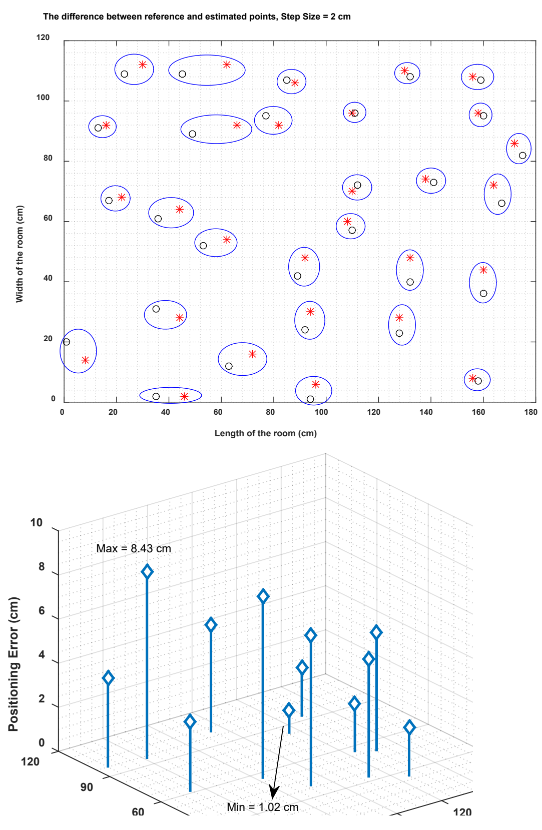

Fig. 5. (top pane) Comparison between reference and estimated points (bottom pane) PE values for different points of the room.

REFERENCES

[1] Chowdhury, M.Z., Hossan, M.T., Islam, A. and Jang, Y.M., 2018. A comparative survey of optical wireless technologies: Architectures and applications. *IEEE Access*, *6*, pp.9819-9840.

[2] Ghassemlooy, Z., Popoola, W. and Rajbhandari, S., 2019. Optical *wireless communications: system and channel modelling with Matlab®*. CRC press.

[3] Ghassemlooy, Z., Arnon, S., Uysal, M., Xu, Z. and Cheng, J., 2015. Emerging optical wireless communications-advances and challenges. *IEEE journal on selected areas in communications*, *33*(9), pp.1738-1749.

[4] Ji, R., Wang, S., Liu, Q. and Lu, W., 2018. High-speed visible light communications: Enabling technologies and state of the art. *Applied Sciences*, *8*(4), p.589.

[5] Khan, F., Jan, S.R., Tahir, M. and Khan, S., 2015, October. Applications, limitations, and improvements in visible light communication systems. In *2015 International Conference on Connected Vehicles and Expo (ICCVE)* (pp. 259-262). IEEE.

[6] Matheus, L.E.M., Vieira, A.B., Vieira, L.F., Vieira, M.A. and Gnawali, O., 2019. Visible light communication: concepts, applications and challenges. *IEEE Communications Surveys & Tutorials*, *21*(4), pp.3204-3237.

[7] Al-Ahmadi, S., Maraqa, O., Uysal, M. and Sait, S.M., 2018. Multi-user visible light communications: State-of-the-art and future directions. *IEEE Access*, *6*, pp.70555-70571.

[8] Pahlavan, K., Li, X. and Makela, J.P., 2002. Indoor geolocation science and technology. *IEEE* Communications *Magazine*, *40*(2), pp.112-118.

[9] Haeberlen, A., Flannery, E., Ladd, A.M., Rudys, A., Wallach, D.S. and Kavraki, L.E., 2004, September. Practical robust localization over large-scale 802.11 wireless networks. In *Proceedings of the 10th annual international conference on Mobile computing and networking* (pp. 70-84).

[10] Liu, J., Chen, R., Pei, L., Guinness, R. and Kuusniemi, H., 2012. A hybrid smartphone indoor positioning solution for mobile LBS. *Sensors*, *12*(12), pp.17208-17233.

[11] Afzalan, M. and Jazizadeh, F., 2019. Indoor positioning based on visible light communication: A performance-based survey of real-world prototypes. *ACM Computing Surveys (CSUR)*, *52*(2), pp.1-36.

[12] Sadowski, S. and Spachos, P., 2018. Rssi-based indoor localization with the internet of things. *IEEE Access*, *6*, pp.30149-30161.

[13] Zhuang, Y., Syed, Z., Li, Y. and El-Sheimy, N., 2015. Evaluation of two WiFi positioning systems based on autonomous crowdsourcing of handheld devices for indoor navigation. *IEEE Transactions on Mobile Computing*, *15*(8), pp.1982-1995.

[14] Hossain, A.M. and Soh, W.S., 2007, September. A comprehensive study of bluetooth signal parameters for localization. In *2007 IEEE 18th International Symposium on Personal, Indoor and Mobile Radio Communications* (pp. 1-5). IEEE.

[15] Ruiz, A.R.J., Granja, F.S., Honorato, J.C.P. and Rosas, J.I.G., 2011. Accurate pedestrian indoor navigation by tightly coupling foot-mounted IMU and RFID measurements. *IEEE Transactions on Instrumentation and measurement*, *61*(1), pp.178-189.

[16] Fang, S.H., Wang, C.H., Huang, T.Y., Yang, C.H. and Chen, Y.S., 2012. An enhanced ZigBee indoor positioning system with an ensemble approach. *IEEE Communications Letters*, *16*(4), pp.564-567.

[17] Zhang, R., Hoflinger, F. and Reindl, L., 2012. Inertial sensor based indoor localization and monitoring system for emergency responders. *IEEE Sensors Journal*, *13*(2), pp.838-848.

[18] Zhuang, Y., Hua, L., Qi, L., Yang, J., Cao, P., Cao, Y., Wu, Y., Thompson, J. and Haas, H., 2018. A survey of positioning systems using visible LED lights. *IEEE Communications Surveys & Tutorials*, *20*(3), pp.1963-1988.

[19] Aminikashani, M., Gu, W. and Kavehrad, M., 2016, January. Indoor positioning with OFDM visible light communications. In *2016 13th IEEE annual consumer communications & networking conference (CCNC)* (pp. 505-510). IEEE.

[20] Lin, B., Tang, X., Ghassemlooy, Z., Li, Y., Zhang, S., Wu, Y. and Li, H., 2016, November. An indoor VLC positioning system based on OFDMA. In *Asia Communications and Photonics Conference* (pp. AS1B-5). Optical Society of America.

[21] Nassiri, M., Ashouri, S., Baghersalimi, G. and Ghassemlooy, Z., 2019. Performance evaluation and comparison of spatial modulation and non-DC MIMO m-CAP techniques in indoor VLC system. *IET Optoelectronics*, *13*(6), pp.281-287.

[22] Olmedo, M.I., Zuo, T., Jensen, J.B., Zhong, Q., Xu, X., Popov, S. and Monroy, I.T., 2013. Multiband carrierless amplitude phase modulation for high capacity optical data links. *Journal of Lightwave Technology*, *32*(4), pp.798-804.

[23] Chvojka, P., Zvanovec, S., Werfli, K., Haigh, P.A. and Ghassemlooy, Z., 2017, May. Variable m-CAP for bandlimited visible light communications. In *2017 IEEE International Conference on Communications Workshops (ICC Workshops)* (pp. 1-5). IEEE.

[24] Nassiri, M., Baghersalimi, G. and Ghassemlooy, Z., 2020. A hybrid VLP and VLC system using m-CAP modulation and fingerprinting algorithm. *Optics Communications*, p.125699.

[25] Werfli, K., Haigh, P.A., Ghassemlooy, Z., Hassan, N.B. and Zvanovec, S., 2016, July. A new concept of multi-band carrier-less amplitude and phase modulation for bandlimited visible light communications. In *2016 10th International Symposium on Communication Systems, Networks and Digital Signal Processing (CSNDSP)* (pp. 1-5). IEEE.

[26] Nassiri, M., Ashouri, S., Baghersalimi, G. and Ghassemlooy, Z., 2018. A comparative performance assessment between pre-equalization and post-equalization techniques in m-CAP indoor VLC systems with bit loading. In *First West Asian Colloquium on Optical Wireless Communications (WACOWC2018)*.

[27] Welch, P., 1967. The use of fast Fourier transform for the estimation of power spectra: a method based on time averaging over short, modified periodograms. *IEEE Transactions on audio and electroacoustics*, *15*(2), pp.70-73.

[28] Kaemarungsi, K., 2005. *Design of indoor positioning systems based on location fingerprinting technique* (Doctoral dissertation, University of Pittsburgh).